

Received May 2, 2019, accepted May 20, 2019, date of publication May 28, 2019, date of current version June 7, 2019.

Digital Object Identifier 10.1109/ACCESS.2019.2919561

Mitigation of Subsynchronous Resonance in Series-Compensated DFIG Wind Farm Using Active Disturbance Rejection Control

YANHUI XU^{ID}, (Member, IEEE), AND SHIMENG ZHAO

School of Electrical and Electronic Engineering, North China Electric Power University, Beijing 102206, China

Corresponding author: Yanhui Xu (xuyanhui23@sohu.com)

This work was supported in part by the National Natural Science Foundation of China (NSFC) under Grant 51677066, in part by the Fund of China Scholarship Council (CSC) under Grant 201806735007, and in part by the Fundamental Research Funds for the Central Universities under Grant 2018MS007 and Grant 2018ZD01.

ABSTRACT This paper presents an active disturbance rejection control (ADRC) method to mitigate subsynchronous resonance (SSR) in a doubly-fed induction generator (DFIG)-based wind farm connected to series compensated transmission lines. First, the frequency of the SSR and its influencing factors are analyzed, and the limitation of the traditional damping controller based on phase compensation is discussed. Then, a damping controller is designed using the ADRC method, which is adapted to the uncertainty SSR frequency of wind farms. The stator current of the DFIG that contain apparent SSR frequency is adopted as the input signals of the ADRC damping controller, and the outputs are added to the current inner loop of the rotor side converter (RSC), which has fast response speed. The performances of the ADRC damping controller are tested in different compensation levels, numbers of DFIG in wind farm, and parameters of the converter control. The simulation results indicate that the ADRC damping controller is superior to the traditional damping controller for mitigating the SSR because it can automatically estimate and compensate the uncertainty disturbances.

INDEX TERMS Active disturbance rejection control, doubly-fed induction generator, rotor side converter, subsynchronous resonance, series capacitor compensation.

I. INTRODUCTION

Doubly-fed induction generator (DFIG) has become a very popular option in wind farms, due to its cost advantage compared with fully rated converter-based wind turbines. Series capacitor compensation is an economical way to increase the power transfer capability of the transmission line connecting the wind farm and the grid. However, the potential risk of subsynchronous resonance (SSR) may cause equipment damage in wind farm or power grid. In 2009, a 345kV transmission line in the southern Electric Reliability Council of Texas (ERCOT) was tripped after a fault, which made the Zorillo Gulf wind farm radically connected to a 50% series compensated line. As a result, SSR with a frequency of about 20 Hz occurred between the DFIG-based wind farm and the series compensated line, which caused a lot of DFIG crowbar circuit damage [1]. Since 2011, the DFIG wind farms located in

the Guyuan area of Hebei Province in China have undergone SSR events hundreds of times caused by interaction between the wind farms and the series compensated lines, of which the oscillation frequency changes from 3 to 10Hz, leading to the abnormal vibration of the transformers and a large number of wind turbines to be disconnected [2]–[4]. Therefore, it is necessary to study the countermeasures for SSR between DFIG wind farm and series compensated lines.

Mitigation of SSR using FACTS such as SVC [5], STATCOM [6], [7], gate-controlled series capacitor [8], [9], and TCSC [5], [10]–[12] have been present. TCSC and SVC are both effective in damping SSR due to torsional interactions as well as induction generator effect (IGE), and TCSC current control is better than SVC in mitigating SSR [5]. Traditional damping controllers based on phase compensation are designed, and the angular velocity or active power is adopted as the input signal [6]–[7]. However, the modification of the wind turbine control system is cheaper than using FACTS and can be quickly implemented. Reference [13]

The associate editor coordinating the review of this manuscript and approving it for publication was Hui Liu.

explores the control capability of DFIG-based wind farms for SSR mitigation, and the dc-link voltage is a valid signal to damp SSR. In literature [14], modulating the reactive power of the GSCs of DFIG is proposed for damping SSR between DFIG-based wind farms and series capacitor compensated transmission systems. The state-space methodology is used to design the SSR damping controller in the literature [15], and the RSC damping control presents a higher damping performance than the GSC damping control. Reference [16] and [17] use the residue-based and root locus methods to find the optimum input control signal and point to introduce the SSR damping controller. A two-degree-of-freedom control strategy is used in the literature [18] to alleviate the SSR. Reference [19] proposes a method to mitigate SSR by embedding subsynchronous notch filters into the converter controllers of DFIGs. A parallel-damping controller is designed based on the rotor torque analysis method in [20]. The literature [21] introduces an active damping strategy to mitigate high-frequency resonance by inserting the virtual impedance to reshape the impedance of the DFIG system. An improved particle swarm optimization algorithm is proposed in reference [22] to optimize the SSR damping controller parameters.

The above SSR damping controllers are mainly designed based on the linearized power system model, which are difficult to tune with the changing atmospheric condition and lack of robustness. So the nonlinear damping controller using partial feedback linearization is proposed to mitigate SSR [23]–[25]. However, the feedback linearization is a model-based nonlinear controller design method, which requires accurate model. Active disturbance rejection control (ADRC) technology is a kind of nonlinear control technology with strong adaptability and robustness. It does not depend on the accuracy of a mathematical model, and all sorts of random uncertain factors in the system are unified into the total disturbance of the system, which can be automatically estimated and compensated [26].

In the existing literature, most of the SSR damping controllers are designed by the phase compensation method. However, the much randomness and variation of the wind farm hindered the extensive use of the traditional damping controller because it may not be useful in some cases. The contributions of this paper are as follows. Firstly, a damping controller is designed using the ADRC method to mitigate SSR in DFIG-based wind farm. The input signals of the ADRC damping controller adopt d-axis and q axis components of stator current, and the outputs are added to the current inner loop of the rotor side converter. Secondly, the small-signal and large disturbance performances of the ADRC damping controller are tested in a simple system with different compensation levels, numbers of DFIG in wind farm, and parameters of converter control. Finally, the feasibility and performance of the ADRC damping controller are checked with a practical system SSR case.

The rest of this paper is organized as follows: Firstly, we analyze the frequency of wind farm SSR and its influence factors in section II. Then in section III, the limitations of

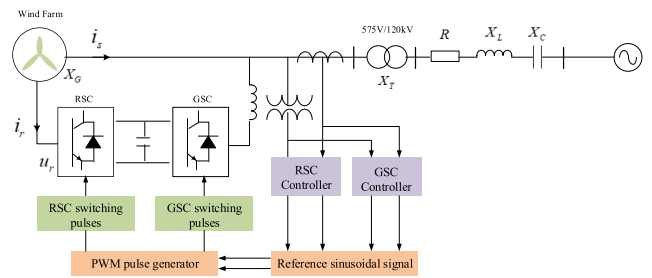


FIGURE 1. DFIG-based series compensated system.

traditional SSR damping controller are analyzed, and the principle of ADRC is introduced. In section IV, the ADRC is used to design the damping controller for mitigating wind farm SSR. The simulations are carried out using MATLAB/SIMULINK to demonstrate the effectiveness of the ADRC damping controller in section V. Section VI concludes the whole paper.

II. THE FREQUENCY OF SSR AND ITS INFLUENCING FACTORS

A. THE FREQUENCY OF SSR

The typical DFIG-based wind farm connecting to the series compensated system is shown in Fig.1.

The degree of compensation is defined as follows:

$$k_c = \frac{X_c}{X_L} \times 100\% \quad (1)$$

where X_C is the capacitance of the series capacitor, X_L is the reactance of the transmission line. Theoretically, the degree of compensation could be 100%. However, its practical limitation is about 80% since a high K_C highlights the problem in protective relays configuration.

In a radial series compensated power system as shown in Fig.1, the electrical resonance frequency is given by

$$f_{er} = f_s \sqrt{\frac{X_c}{X_{L\Sigma}}} \quad (2)$$

where f_s is the synchronous frequency, $X_{L\Sigma}$ is the sum of the equivalent reactance of the wind farm, transformer, and transmission line. The equivalent degree of compensation is defined as followed:

$$k_{ec} = \frac{X_c}{X_{L\Sigma}} \times 100\% \quad (3)$$

Since the reactance of the generator and transformer is larger than the reactance of the transmission line, the equivalent compensation degree is much lower than 80%.

For a wind farm consisting of identical DFIGs, if we neglect concentrating network, the electrical resonance frequency is given by

$$f_{er} = f_s \sqrt{\frac{k_c X_L}{X_G/n + X_T + X_L}} \quad (4)$$

where n is the number of DFIG, X_G is the reactance of one DFIG, X_T is the reactance of the transformer.

According to the theory of the rotation generator, the oscillation frequency of the active power is complementary to the resonance frequency of the stator current [4].

$$f_p = f_s - f_{er} \tag{5}$$

where f_p is the oscillation frequency of the active power.

For the IGE phenomenon, the above frequency relationships are sufficient. However, sub-synchronous control interaction (SSCI) is much more complex than IGE. SSCI is mainly due to the interactions between DFIG wind turbine controllers and the series compensated transmission line. The mechanism of SSCI can be interpreted as follows.

1) When a disturbance occurred in the DFIG-based series compensated system, distorted voltages and currents containing electrical resonance frequency components are measured and fed to the controllers.

2) The RSC and GSC controllers process the distorted information, and the output signals of the controllers are adjusted.

3) The above output signals are fed to the PWM pulse generator and contain sub-synchronous distortion, which may intensify the sub-synchronous components in the stator.

4) The closed-loop system response, including the series compensated line, the RSC and GSC controllers and the DFIG converters, has negative damping, leading to SSCI.

B. INFLUENCING FACTORS OF THE SSR FREQUENCY

According to the above analysis, the frequency of SSR depends not only on the configuration of the series compensated transmission line and induction generator parameters but also on the wind turbine controller configuration and parameters.

Taking the DFIG-based series compensated system in Fig.1 as an example, the detailed parameters given in Appendix A Table 1, we analyze the influence of the degree of series compensation, the number of DFIG, the RSC and GSC controller proportional gains on the frequency of SSR as shown in Fig.2.

From Fig.2, we can find that the frequency of SSR is mainly relative to the degree of series compensation k_c , the number of DFIG n and the RSC proportional coefficient k_{p_rsc} . The GSC proportional coefficient k_{p_gsc} has little effect on the frequency of SSR.

III. THE TRADITIONAL DAMPING CONTROLLER AND THE ADRC METHOD

A. THE TRADITIONAL DAMPING CONTROLLER AND ITS LIMITATION

The damping coefficient D_e of DFIG can be expressed as

$$D_e = \text{Re}(\Delta T_e / \Delta \omega) \tag{6}$$

where ΔT_e and $\Delta \omega$ are the increments of electromagnetic torque and the speed of rotor respectively. When the phase

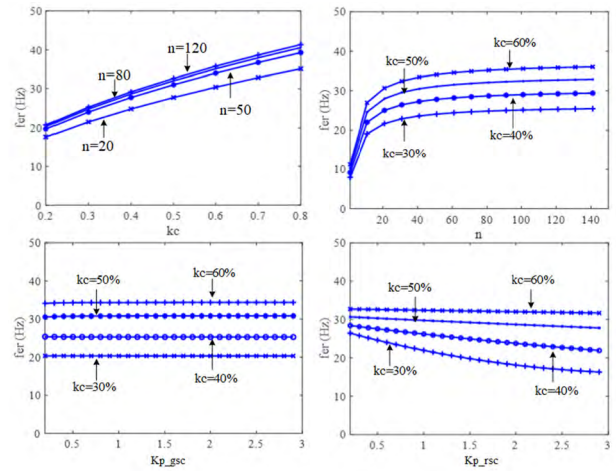


FIGURE 2. The relationship of the SSR frequency with the wind turbine and grid parameters.

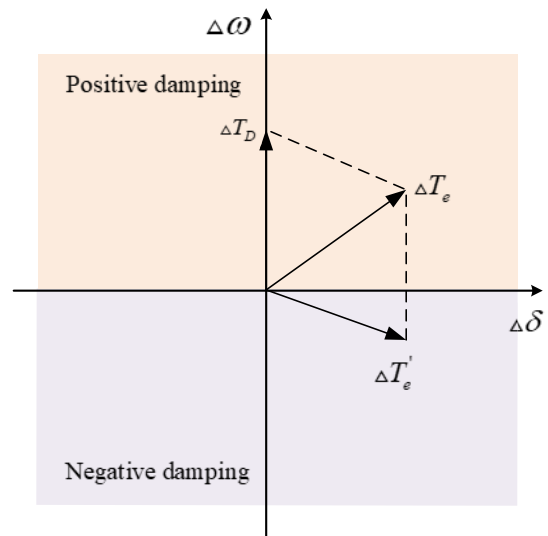


FIGURE 3. Vector diagram of the electromagnetic torque.

difference between the increments of electromagnetic torque and the speed of the rotor exceeds 90° , a negative damping effect will occur, as shown by $\Delta T_e'$ in Fig.3. The purpose of traditional damping controller is to generate a purely positive damping torque ΔT_D making the negative damping torque $\Delta T_e'$ become the positive damping torque ΔT_e .

The common suppression strategies use an additional damping controller, which can be added to the active power outer loop of the RSC. Select the speed deviation $\Delta \omega$ as the input of the controller, generate the output signal ΔP_f through the band-pass filtering, phase shifting link and the gain, and add it to active power outer loop of the rotor side to generate an additional electromagnetic torque to suppress SSR. Its structure is as follows.

The traditional damping controller mainly depends on the phase shifting link to provide phase compensation. As a result, the damping torque becomes positive to mitigate SSR [18], [21]. But the phase shifting link is effective for

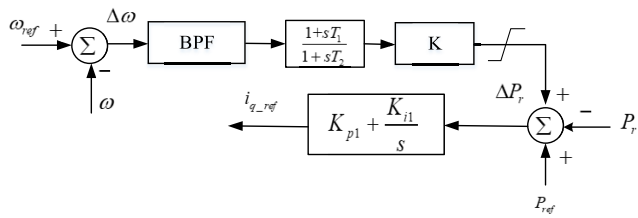


FIGURE 4. The structure diagram of the traditional damping controller.

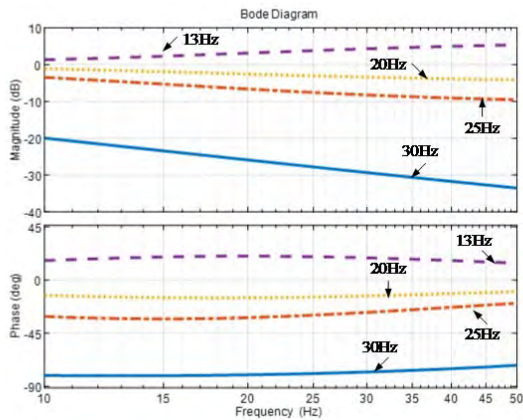


FIGURE 5. Bode diagram of the phase shifting link.

a given frequency extent. Due to the considerable variation of SSR frequency in wind farm, the function of traditional damping controller will be limited. We only draw the Bode diagram of the phase shifting link as follows.

It can be found from the Fig.5 that when frequencies of the subsynchronous oscillation in the system differ significantly, the phase-frequency characteristics of the phase shifting link vary greatly. For example, when the parameters are designed for a subsynchronous oscillation frequency of 30 Hz, the desired phase compensation can be achieved, resulting in positive damping. However, when the oscillation frequency becomes 13 Hz, if the phase shifting link still uses the original parameters, the phase compensation will cause a significant deviation, and negative damping will occur. It is noted that if the oscillation frequency of the wind power changes considerably, the traditional damping controller designed for a specific situation may be ineffective or even exacerbate the oscillation.

To solve this problem, this paper applies the ADRC method to mitigate SSR. The factors influencing SSR frequency will be taken as disturbances, and ADRC can timely estimate and compensate these disturbances so that the SSR of the wind farm can be mitigated.

B. THE ADRC METHOD

The complete structure of the ADRC is shown in Fig.6.

The ADRC is composed of a tracking differentiator (TD), a nonlinear state error feedback (NLSEF), an extended state observer (ESO), and a disturbance estimation

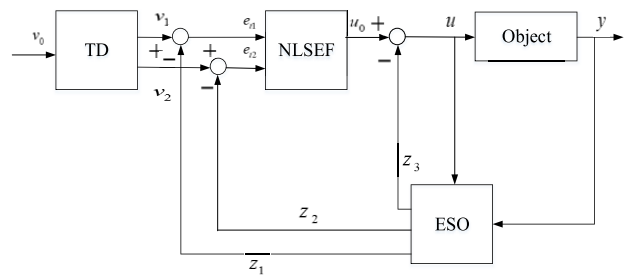


FIGURE 6. The structure diagram of the ADRC.

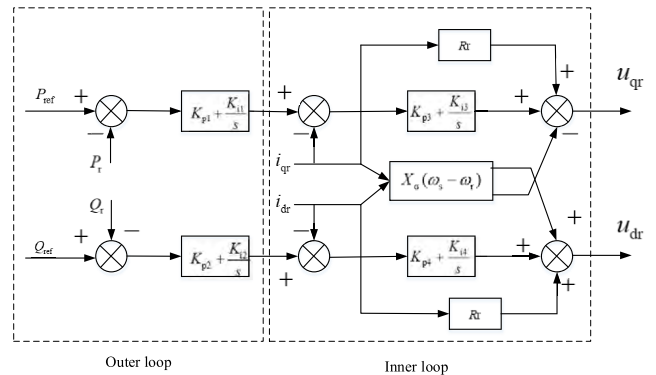


FIGURE 7. The control strategy of the rotor side converter.

compensation [26]. The core of ADRC’s control is dynamic estimation and compensation of the sum disturbance, and the state variable motion model of the controlled object determines the feedback control. Firstly, the disturbance that can affect the controlled output is expanded into a new state variable by the ESO.

Set the second-order nonlinear system as

$$\begin{cases} \dot{x}_1 = x_2 \\ \dot{x}_2 = f(x_1, x_2) + bu \\ y = x_1 \end{cases} \quad (7)$$

where y is the output of the system, and u is the input of the system; $f(x_1, x_2)$ is the function of both the model of controlled object and external disturbances. Let $x_3 = f(x_1, x_2)$, which is expanded into a new state variable, and define it as a total disturbance. In the content of feedback control, it is something that needs to be overcome by the control signal. Therefore, we turn the model definition into a disturbance compensation problem. Let

$$\dot{x}_3(t) = G(t) \quad (8)$$

The (7) can be described as

$$\begin{cases} \dot{x}_1 = x_2 \\ \dot{x}_2 = x_3 + bu \\ \dot{x}_3 = G(t) \\ y = x_1 \end{cases} \quad (9)$$

We establish a state observer for the system as follows.

$$\begin{cases} \dot{e}_1 = z_1 - y \\ \dot{z}_1 = z_2 - \beta_{01}g_1(e_1) \\ \dot{z}_2 = z_3 - \beta_{02}g_2(e_1) + bu \\ \dot{z}_3 = -\beta_{03}g_3(e_1) \end{cases} \quad (10)$$

where z_1, z_2 are the estimated values of the ESO for the system state variables x_1, x_2 , and z_3 is an estimated value of the total disturbance x_3 ; e_1 is the error, and $\beta_{01}, \beta_{02}, \beta_{03}$ are proportional coefficients; The function $g_n(e_1)$ is the selected nonlinear function, set

$$g_n(e_1) = |e_1|^{\frac{1}{2n-1}} \text{sign}(e_1) \quad (11)$$

Let $e_1 = z_1 - x_1, e_2 = z_2 - x_2$ and $e_3 = z_3 - x_3$. When $G(t) = g_0$, the error equation is

$$\begin{cases} \dot{e}_1 = e_2 - \beta_{01}g(e_1) \\ \dot{e}_2 = e_3 - \beta_{02}g_2(e_1) \\ \dot{e}_3 = g_0 - \beta_{03}g_3(e_1) \end{cases} \quad (12)$$

When the system enters a steady state, the right end of the equation converges to zero. It explains that as long as the parameters are properly selected, the system can track and eliminate errors very well without knowing the specific expression of the controlled object.

The working principle of the ADRC suppressing SSR is as follows. When SSR occurs, the ESO will produce the estimated state variables z_1, z_2 , and total disturbance z_3 of the system according to the input y and control signal u . With the stator current reference v_0 , the TD arranges a suitable transition process v_1 and extracts the differential signal v_2 in order to track the input signal as soon as possible. Then the NLSEF uses the state error signals e_1, e_2 to generate the error feedback control u_0 . Finally, the control signal u is formed through the estimation and compensation of the total disturbance, which is added to the current inner loop control of RSC as an additional control signal to mitigate SSR.

The complete ADRC algorithm is as follows, which is the specific mathematical expression of the ADRC. The order of this formula is based on TD, ESO, NLSEF, and the dynamic compensation.

$$\begin{cases} fh = fhan(v_1 - v_0, v_2, r_0, h) \\ v_1 = v_1 + hv_2 \\ v_2 = v_2 + hfh \\ e = z_1 - y, fe = fal(e, 0.5, h), fe_1 = fal(e, 0.25, h) \\ z_1 = z_1 + h(z_2 - \beta_{01}e) \\ z_2 = z_2 + h(z_3 - \beta_{02}fe + u) \\ z_3 = z_3 + h(-\beta_{03}fe_1) \\ e_1 = v_1 - z_1, e_2 = v_2 - z_2 \\ u_0 = -fhan(e_1, ce_2, r, h_1) \\ u = u_0 - z_3 \end{cases} \quad (13)$$

where h is the sampling step, r is the velocity factor, and h_1 is the filtering factor. The *fhan* is the fastest control synthesis function, and we use it for feedback control. In the TD and disturbance compensation, it can eliminate the overshoot in the speed curve, which can well suppress the noise amplification in the differential signal. The *fal* is a continuous power function with a linear segment near the origin, which can avoid high frequency chattering in ESO. The specific form of the two functions has been placed in the appendix B. As to the reason why the effects of the two functions above can achieve, it is explained in [26].

In the DFIG-based series compensated system, due to natural reasons such as wind speed, the wind power output has high volatility and randomness, and the uncertainty of the load will make the operating condition of the system change regularly. The subsynchronous oscillation problem will be affected by this change. According to the analysis of influencing factors on SSR frequency in section II, the degree of series compensation, the number of DFIG, and the proportional gain of RSC will have a significant effect on SSR frequency. ADRC can unify all kinds of uncertain factors in the system into the total disturbance of the system regardless of any form of the mathematical model, using the ESO to estimate the state variable in real time automatically and dynamically compensate for eliminating the effect of disturbance, thereby mitigating SSR under different operating manners in the wind farm [27].

C. THE IMPROVEMENT OF THE ADRC METHOD TO THE PID CONTROL IN SSR SUPPRESSION

The traditional damping controller mostly adopts the PID control, which can achieve good performance under certain conditions. However, the PID based controller requires an accurate model of the controlled object. The wind power system is a strong nonlinear time-varying system, and it has high randomness. Therefore, the accurate model of the wind farm is difficult to acquire. Moreover, the oscillation frequency may change with the disturbances at any time, which makes the application of the traditional damping controller limited, and cannot suppress SSR under the multi-state operation of the wind system.

The ADRC is different from the PID controller in the working principle. The ADRC only needs to meet the requirements that track the disturbance input fast and accurately and minimize the error. At the same time, the ESO of the ADRC treats all the internal and external variations as the total disturbance and expands it into a new state variable. By this means, the ADRC realized automatic estimation and compensation without knowing the specific expression of the controlled object and the disturbance. Consequently, it is not necessary for the ADRC to know the oscillation frequency of SSR. The specific explanations in principle are as follows.

The equation of the d-axis rotor current is

$$\frac{di_{dr}}{dt} = x_3 + bu_{dr} \quad (14)$$

where x_3 is the total disturbance, including the operating state of the DFIG and the sub-synchronous disturbance information. The (7) can be expressed as

$$\begin{cases} \dot{x}_1 = x_2 \\ \dot{x}_2 = x_3 + bu_{dr} \\ y = x_1 = i_{dr} \end{cases} \quad (15)$$

According to the error expression in (12), when the whole system enters the steady state, the equation should converge to zero.

$$\begin{cases} e_2 - \beta_{01}e_1 = 0 \\ e_3 - \beta_{02}|e_1|^{\frac{1}{2}}\text{sign}(e_1) = 0 \\ g_0 - \beta_{03}|e_1|^{\frac{1}{4}}\text{sign}(e_1) = 0 \end{cases} \quad (16)$$

Therefore, the steady state error of the system is

$$|e_1| = \left(\frac{g_0}{\beta_{03}}\right)^4, |e_2| = \beta_{01}\left(\frac{g_0}{\beta_{03}}\right)^4, |e_3| = \beta_{02}\left(\frac{g_0}{\beta_{03}}\right)^2 \quad (17)$$

These estimation errors are small enough as long as β_{03} is much greater than g_0 . It is proved that regardless of the disturbance form, as long as its action amount in the process is bounded, we can always choose the parameters reasonably, so that the ESO can estimate the state of the controlled object well and minimize the error.

According to the ADRC algorithm of (13) and the specific expression in the appendix, the final additional control signal can be expressed as

$$\begin{aligned} \Delta u_{dr} &= u_0 - z_3 \\ &= -fhan(v_1 - z_1, c(v_2 - z_2), r, h_1) - z_3 \end{aligned} \quad (18)$$

We can find that it is independent of the frequency of SSR and the specific expression of the disturbance. So the ADRC can accurately and quickly compensate for the sub-synchronous disturbance. Even if the operating state of the wind power system changed, the ADRC still could provide sufficient damping to mitigate the SSR.

IV. DESIGN OF THE ADRC DAMPING CONTROLLER

The DFIG provides the excitation voltage through the rotor side converter, which also decouples the active and reactive power output of the generator. The entire controller consists of current inner loop control and a power outer loop control [10], [12]. The control block diagram is as follows.

To effectively mitigate the SSR of the DFIG-based wind farm, this paper uses ADRC control to replace the phase shifting link and gain of the traditional damping controller, as shown in Fig.4. The specific design block diagram of the ADRC-based damping controller is as follows.

According to the mechanism analysis above, when the SSR phenomenon occurs, the stator current of DFIG contains the subsynchronous resonant component. Although the speed deviation also contains SSR information, the stator current is more directly affected by SSR and has more abundant frequency spectrum information. On the other hand, the input of the ADRC and the output of the controlled object need

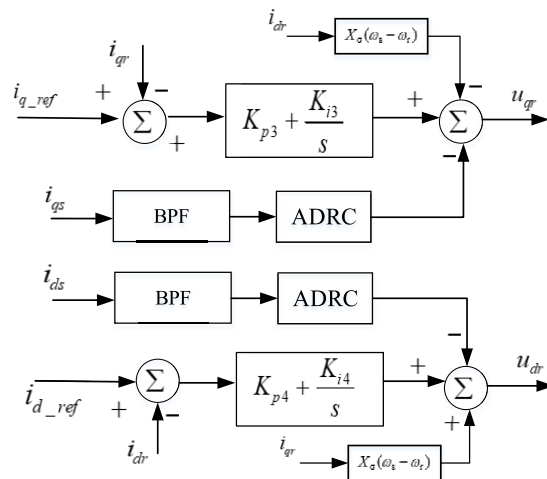


FIGURE 8. The ADRC damping controller.

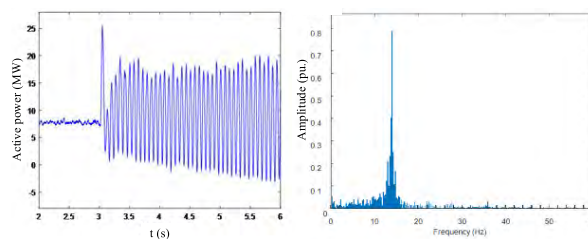


FIGURE 9. Active power response without damping controller.

to adopt the same type variable. Therefore, the disturbing component of the stator current is extracted as the input of the ADRC damping controller. In order to eliminate the influence of the steady-state DC component, a Butterworth band-pass filter is used, and the ADRC damping control does not affect the transfer function with power frequency. At the same time, regarding response time and speed, the power loop is the outer loop, of which the dynamic response time is long, but the current loop is the inner loop, of which the response speed is fast. To achieve fast-tracking of the current reference value, the output of the controller is added to the current inner loop of the rotor side converter, and the output voltage of the rotor is adjusted. Finally, the damping torque can be generated to mitigate the SSR phenomenon.

The corresponding relationship between the input and output quantities of the ADRC method and the additional control quantity is: the input value v_0 of the ADRC is the stator current reference i_{qs} and i_{ds} of DFIG; the output u of the ADRC is the rotor voltage, which is the quantity that we want to control by adding ADRC damping control; the input signal y of ESO is the stator current, that is estimated and compensated for the fast tracking of i_{qs} and i_{ds} . The ADRC controller has many parameters. The speed factor r and the sampling step h are basic parameters, β_{01} , β_{02} , β_{03} are the gain coefficients in the ESO, and the nonlinear state error feedback parameter is c . The parameters of each part can be adjusted according to the principle of separation [26]. Since ADRC performance has a small dependence on settings,

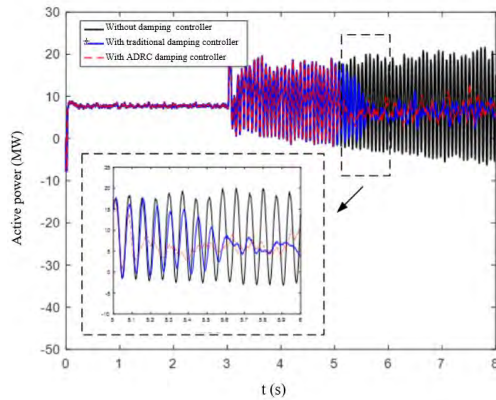


FIGURE 10. Active power responses with different damping controller.

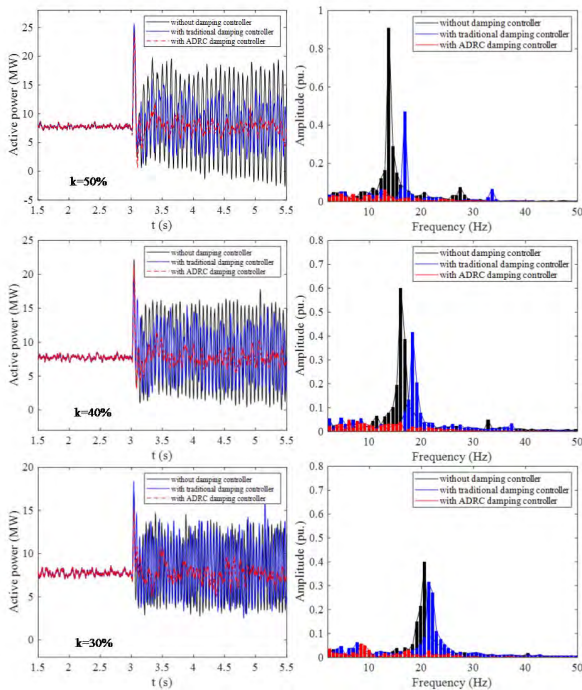


FIGURE 11. Active power responses under different degree of series compensation.

it possesses strong adaptability and robustness, which means that most parameters can achieve better results after simple tuning. In this paper, we take $c = 0.5$ and $r = 0.5/h^2$. There are many ways to choose $\beta_{01}, \beta_{02}, \beta_{03}$. Here, we set $\beta_{01} = 1/h, \beta_{02} = 1/3h^2$, and $\beta_{03} = 1/32h^3$.

V. TIME DOMAIN SIMULATION ANALYSIS

To demonstrate the effectiveness of the ADRC damping controller, the simulation platform of the DFIG-based series compensated system shown in Fig.1 is put up using Matlab/Simulink. The rated power of DFIG is set to 1.5MW, the voltage of the connection point of DFIG is 575V, the wind speed is set to 12m/s, and the equivalent degree of series compensation is 55%. The series compensated capacitor is added

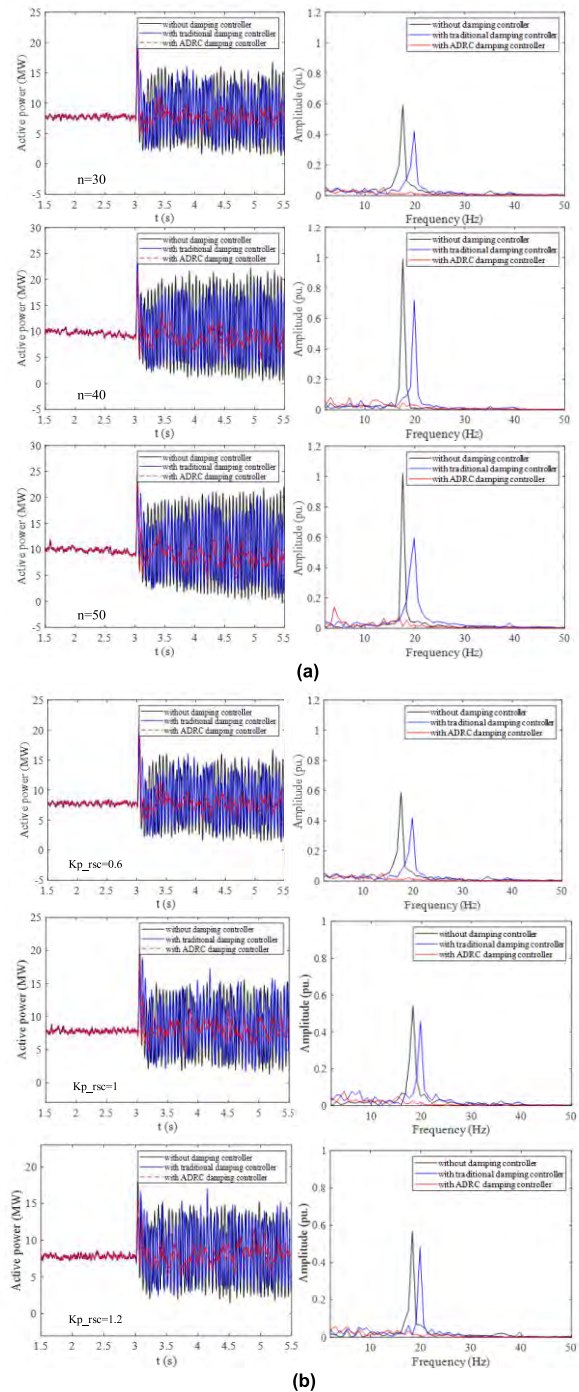


FIGURE 12. Active power responses under different parameters of DFIG. (a) Different number of the DFIG. (b) Different proportion coefficient of the RSC.

at $t = 3s$. When there is no damping controller, the line active power response characteristics are shown in the Fig.9.

It can be seen from the Fig.9 that when there is no damping controller, the SSR phenomenon occurs after the series compensated capacitors put into use, and active power begins to diverge. By performing spectrum analysis on the active power, the oscillation frequency is about 13 Hz.

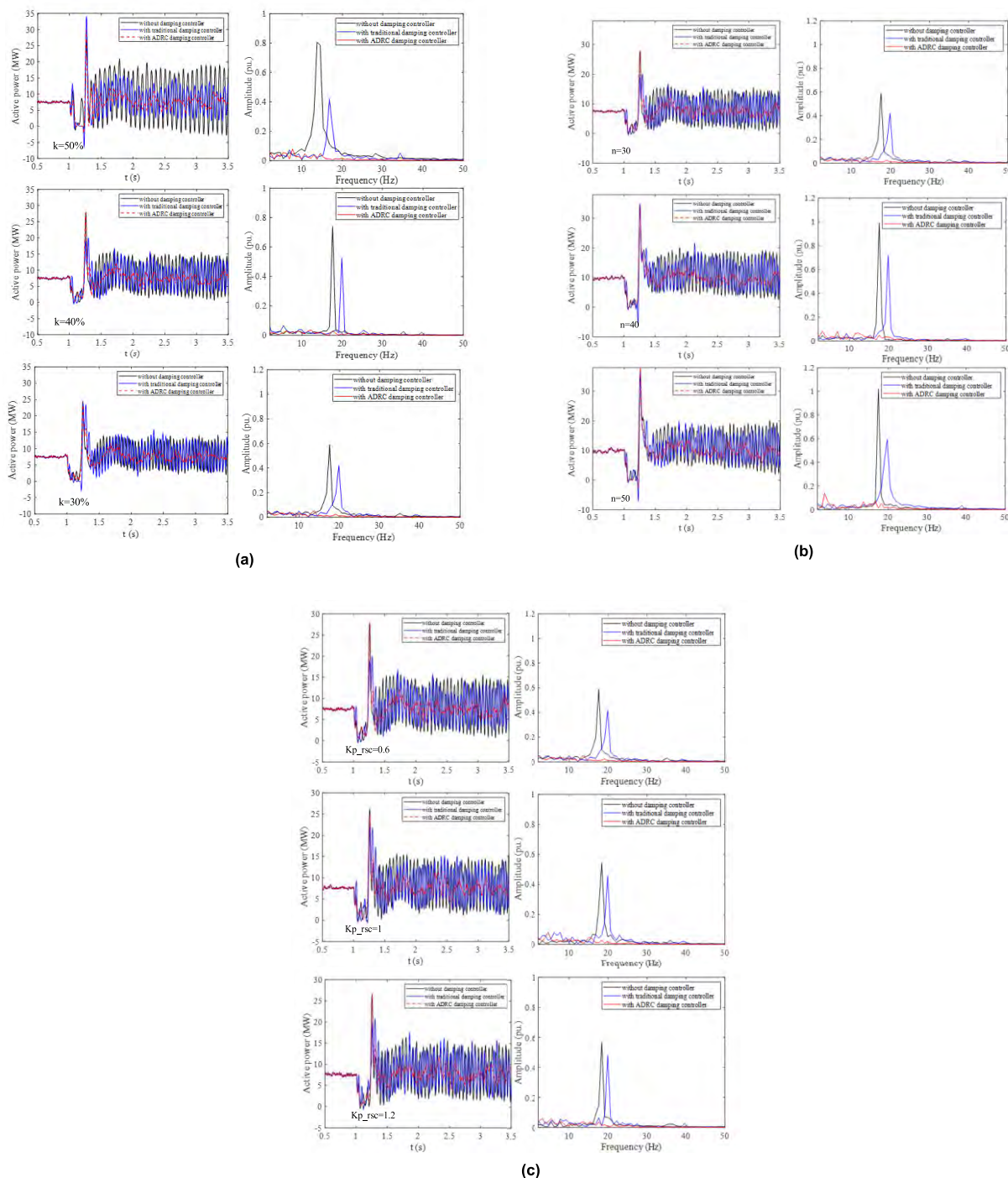


FIGURE 13. Active power responses with different damping controller under the three-phase short-circuit fault. (a) Different degree of series compensation. (b) Different number of DFIG. (c) Different proportion coefficient of RSC.

While maintaining the conditions above, the traditional damping controller and the ADRC damping controller is separately applied at $t = 5$ s, and the simulation results are as follows.

It can be seen from the Fig.10 that after adding the traditional or the ADRC damping controller, both can provide sufficient positive damping for mitigating SSR. It is

indicated that the traditional damping controller designed for this frequency can still have a good mitigating effect, which is not much different from the ADRC controller, but the latter's convergence speed is faster. Next, we study the output response of DFIG with traditional damping controller and the ADRC damping controller under different conditions.

A. DIFFERENT DEGREE OF SERIES COMPENSATION

Change the equivalent degree of series compensation of the line and observe the response of the active power of the line under different damping controllers.

It can be seen from Fig. 11 that after the series compensated capacitor is added at $t = 3s$, the system without damping controller exhibits a divergent or equal amplitude oscillation state. After adding the traditional damping controller, the oscillation can be attenuated to some extent, but the effect is not good. Due to the change of the degree of series compensation, the SSR frequency of the system is shifted. The traditional damping controller is sensitive to the frequency, and the parameters cannot be adjusted according to the real-time operating state of the system, which makes the mitigating effect of the traditional controller designed for specific operating conditions is not effective. The ADRC damping controller can perform real-time estimation and feedback compensation for the disturbance, and quickly suppress the SSR. Its mitigating effect is less affected by the change of the degree of series compensation, which can ensure the stable power transmission of the system, showing its good adaptability, and it is consistent with the theoretical analysis in section III.

B. DIFFERENT PARAMETERS OF THE DFIG

Observe the response characteristics of the line active power under a different number of DFIG and the RSC parameters, and compare the mitigating effect of the traditional damping controller and the ADRC.

From Fig. 12, we can see that the ADRC damping controller can achieve better results under different numbers of the wind turbine and RSC control parameters, reflecting its adaptability and robustness to system operating conditions and model parameters. However, when the traditional damping controller is out of the adjusted situation, it is challenging to mitigate SSR, and the parameters may need to be re-tuned.

The simulation results show that the proposed ADRC damping controller has strong robustness, and is less affected by the operating state of DFIG, and exhibits good anti-interference ability when the parameters change. It has strong adaptability and good mitigating effect, ensuring stable operation of the system.

C. PERFORMANCE OF THE ADRC UNDER LARGE DISTURBANCE

The transient response of the system is evaluated by applying a 200-ms three-phase short-circuit fault in the series-compensated transmission line, and the fault occurs at $t=1s$. The simulation results with and without damping controllers are presented as follows.

The simulation results show that the ADRC damping controller also has good mitigating effect under a large disturbance, which proves its strong robustness and good anti-interference ability when the parameters change, ensuring stable operation of the system.

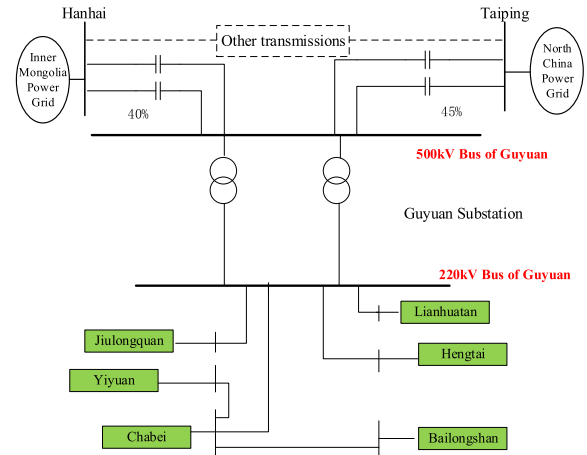


FIGURE 14. Diagram of wind farms integration in Guyuan area.

D. PERFORMANCE OF THE ADRC WITH A PRACTICAL SYSTEM

In this paper, a practical wind-farm system locating in Guyuan, Hebei Province, China is adopted to check the performance of the ADRC damping controller as shown in Fig. 14.

There are six large-scale wind farms, namely Lianhuan, Jiulongquan, Bailongshan, Hengtai, Chabei, and Yiyuan. These wind farms are collected by transformers of 0.69/35/220 kV, then connected to the main grid of North China and Inner Mongolia through 500kV transmission lines with 45% or 40% series compensation respectively.

Subsynchronous resonance has been detected many times in Guyuan area since 2010. Only from the end of 2012 to the end of 2013, as many as 58 oscillation events occurred. The resonant frequency of the current is about 6 to 8 Hz, and an equivalent electric circuit is deduced to explain why SSR happens in [2]. The [3] has demonstrated that the converter control of DFIG produces negative resistance at the slip frequency and thus causes unstable SSR. An improved impedance method using aggregated RLC circuit model is proposed in [4] and applied for SSR analysis of Guyuan area. Subsynchronous notch filters are embedded into DFIG converter controllers to mitigate SSR and applied to Guyuan area series-compensated wind-farm system as a case study [19]. To test the performance of the ADRC damping controller with the practical system above, we set the wind speed of 8m/s and 1500 identical 1.5MW DFIGs online. The specific parameters of transmission lines are the same as that in [19] and are listed in Appendix A Table 2. The series compensations are put in at $t = 2s$. The time domain simulation results with and without mitigating measures are as follows.

According to (5) in section II, the frequency of active power is complementary to the resonance frequency of stator current, so the simulation results as shown in Fig. 15 are identical to that of [19] from frequency characteristic point of view. It can be seen that the ADRC damping controller has good potential in mitigating SSR of practical systems.

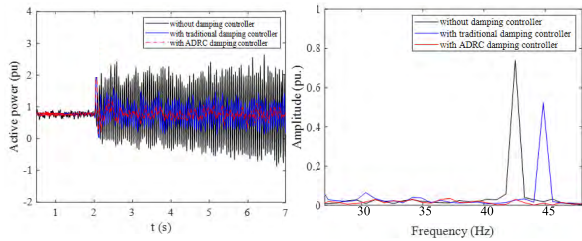


FIGURE 15. The 220kV-side active power of the transformers at Guyuan substation.

TABLE 1. The main parameters of the system.

Name	Symbol	Value
Rated power of DFIG	S_G	1.5MW
Voltage reference of grid side	V_t	575V
Equivalent inductance of line	L	0.0315H/km
Resistance of line	R	0.1153Ohms/km
Inductance of transformer	L_t	0.025pu.
The stator resistance of DFIG	R_s	0.023pu.
The stator inductance of DFIG	L_s	0.18pu.
The rotor resistance of DFIG	R_r	0.016pu.
The rotor inductance of DFIG	L_r	0.16pu.
The proportional gain of RSC	K_{p_rsc}	0.6
The proportional gain of GSC	K_{p_gsc}	0.83

VI. CONCLUSION

To mitigate the SSR of DFIG-based wind farm connecting to the series compensated system, this paper presents a damping controller design based on ADRC. Through theoretical analysis and time domain simulation, the following conclusions are arrived at.

- 1) The frequency of SSR has a considerable variation with the series compensation level, the number of DFIG in wind farm and the parameter of RSC control, which will make the traditional damping controller invalid in some cases.
- 2) The ADRC damping controller added to the current inner loop of RSC can automatically estimate the state variable in real time and dynamically compensate for eliminating the effect of disturbance.
- 3) The ADRC damping controller has stronger adaptability than traditional damping controller, which can effectively mitigate SSR of the DFIG based wind farm under different operating conditions.
- 4) The ADRC has more parameters than the traditional PID controller. Therefore, how to simplify the parameters setting of the ADRC should be the focus of future research.

APPENDIX A

See Table 1 and 2.

TABLE 2. Parameters of transmission lines in the practical system of Guyuan.

Transmission lines	Length (km)	Resistance (Ω /km)	Reactance (Ω /km)
GY-TP	272	0.016	0.2
GY-HH	193	0.016	0.2
GY-JYQ	24.6	0.074	0.39
GY-HT	24.7	0.032	0.24
GY-LHT	71.3	0.02	0.16
GY-CB	65	0.018	0.26
BLS-CB	67	0.023	0.29
YY-CB	106	0.023	0.29

APPENDIX B

The complete algorithm for the ADRC method with disturbance tracking compensation is as follows.

- 1) Arrange the transition process with the set value v_0 as input

$$\begin{cases} e = v_1 - v_0 \\ fh = fhan(e, v_2, r_0, h) \\ v_1 = v_{10} + hv_2 \\ v_2 = v_{20} + hfh \end{cases}$$

The fastest control integrating function is recorded as $fhan(x_1, x_2, r, h)$. Its algorithm formula is as follows.

$$\begin{cases} u = fhan(x_1, x_2, r, h) \\ d = rh \\ d_0 = hd \\ y = x_1 + hx_2 \\ a_0 = \sqrt{d^2 + 8r|y|} \\ a = \begin{cases} x_2 + \frac{(a_0 - d)}{2} \text{sign}(y), & |y| > d_0 \\ x_2 + \frac{y}{h}, & |y| \leq d_0 \end{cases} \\ fhan = - \begin{cases} r \text{sign}(a), & |a| > d \\ r \frac{a}{d}, & |a| \leq d \end{cases} \end{cases}$$

where d, d_0 are the length of the linear segment of the function $fhan$, and y, a, a_0 are internal variables.

- 2) Track and estimate the status and disturbance of the system with the system output y and input u

$$\begin{cases} e_1 = z_1 - y, fe = fal(e_1, 0.5, \delta), fe' = fal(e_1, 0.25, \delta) \\ z_1 = z_{10} + h(z_2 - \beta_{01}e_1) \\ z_2 = z_{20} + h(z_3 - \beta_{02}fe + u) \\ z_3 = z_{30} + h(-\beta_{03}fe') \end{cases}$$

In the formula, $\beta_{01}, \beta_{02}, \beta_{03}$ are a set of parameters. The function fal is

$$\begin{aligned} fal(x, \alpha, \delta) &= \frac{x}{\delta^{1-\alpha}} f_{sg}(x, \delta) + |f_{db}(x, \delta)| |x|^\alpha \text{sign}(x) \\ f_{sg}(x, \delta) &= \frac{\text{sign}(x + \delta) - \text{sign}(x - \delta)}{2} \\ f_{db}(x, \delta) &= \frac{\text{sign}(x + \delta) + \text{sign}(x - \delta)}{2} \end{aligned}$$

where α is a power function, δ is the the length of the linear segment, and sign is the symbol function.

3) The state error feedback law is

$$\begin{cases} e_{t1} = v_1 - z_1, e_{t2} = v_2 - z_2 \\ u_0 = -fhan(e_{t1}, ce_{t2}, r, h_1) \end{cases}$$

4) The process of disturbance compensation is

$$u = u_0 - z_3$$

REFERENCES

- [1] G. D. Irwin, A. K. Jindal, and A. L. Isaacs, "Sub-synchronous control interactions between type 3 wind turbines and series compensated AC transmission systems," in *Proc. IEEE Power Energy Soc. Gen. Meeting*, Jul. 2011, pp. 1–6.
- [2] L. Wang, X. Xie, Q. Jiang, H. Liu, Y. Li, and H. Liu, "Investigation of SSR in practical DFIG-based wind farms connected to a series-compensated power system," *IEEE Trans. Power Syst.*, vol. 30, no. 5, pp. 2772–2779, Sep. 2015.
- [3] X. Xie, X. Zhang, H. Liu, H. Liu, Y. Li, and C. Zhang, "Characteristic analysis of subsynchronous resonance in practical wind farms connected to series-compensated transmissions," *IEEE Trans. Energy Convers.*, vol. 32, no. 3, pp. 1117–1126, Sep. 2017.
- [4] H. Liu, X. Xie, C. Zhang, Y. Li, H. Liu, and Y. Lu, "Quantitative SSR analysis of series-compensated DFIG-based wind farms using aggregated RLC circuit model," *IEEE Trans. Power Syst.*, vol. 32, no. 1, pp. 474–483, Jan. 2017.
- [5] R. K. Varma, S. Auddy, and Y. Semsedini, "Mitigation of subsynchronous resonance in a series-compensated wind farm using FACTS controllers," *IEEE Trans. Power Del.*, vol. 23, no. 3, pp. 1645–1654, Jul. 2008.
- [6] M. S. El-Moursi, B. Bak-Jensen, and M. H. Abdel-Rahman, "Novel STATCOM controller for mitigating SSR and damping power system oscillations in a series compensated wind park," *IEEE Trans. Power Electron.*, vol. 25, no. 2, pp. 429–441, Feb. 2010.
- [7] A. Moharana, R. K. Varma, and R. Seethapathy, "SSR Alleviation by STATCOM in induction-generator-based wind farm connected to series compensated line," *IEEE Trans. Sustain. Energy*, vol. 5, no. 3, pp. 947–957, Jul. 2014.
- [8] H. A. Mohammadpour, A. Ghaderi, and E. Santi, "Analysis of sub-synchronous resonance in doubly-fed induction generator-based wind farms interfaced with gate-controlled series capacitor," *IET Gener., Transmiss. Distrib.*, vol. 8, no. 12, pp. 1998–2011, Dec. 2014.
- [9] H. A. Mohammadpour and E. Santi, "Modeling and control of gate-controlled series capacitor interfaced with a DFIG-based wind farm," *IEEE Trans. Ind. Electron.*, vol. 62, no. 2, pp. 1022–1033, Feb. 2015.
- [10] H. Xie, B. Li, C. Heyman, M. M. De Oliveira, and M. Monge, "Sub-synchronous resonance characteristics in presence of doubly-fed induction generator and series compensation and mitigation of subsynchronous resonance by proper control of series capacitor," *IET Renew. Power Gener.*, vol. 8, no. 4, pp. 411–421, May 2014.
- [11] L. Piyasinghe, Z. Miao, J. Khazaei, and L. Fan, "Impedance model-based SSR analysis for TCSC compensated type-3 wind energy delivery systems," *IEEE Trans. Sustain. Energy*, vol. 6, no. 1, pp. 179–187, Jan. 2015.
- [12] A. Adrees and J. V. Milanović, "Optimal compensation of transmission lines based on minimization of the risk of subsynchronous resonance," *IEEE Trans. Power Syst.*, vol. 31, no. 2, pp. 1038–1047, Mar. 2016.
- [13] L. Fan and Z. Miao, "Mitigating SSR using DFIG-based wind generation," *IEEE Trans. Sustain. Energy*, vol. 3, no. 3, pp. 349–358, Jul. 2012.
- [14] U. Karaagac, S. O. Faried, J. Mahseredjian, and A.-A. Edris, "Coordinated control of wind energy conversion systems for mitigating subsynchronous interaction in DFIG-based wind farms," *IEEE Trans. Smart Grid*, vol. 5, no. 5, pp. 2440–2449, Sep. 2014.
- [15] A. E. Leon and J. A. Solsona, "Sub-synchronous interaction damping control for DFIG wind turbines," *IEEE Trans. Power Syst.*, vol. 30, no. 1, pp. 419–428, Jan. 2015.
- [16] H. A. Mohammadpour and E. Santi, "Optimal adaptive sub-synchronous resonance damping controller for a series-compensated doubly-fed induction generator-based wind farm," *IET Renew. Power Gener.*, vol. 9, no. 6, pp. 669–681, Aug. 2015.
- [17] H. A. Mohammadpour and E. Santi, "SSR damping controller design and optimal placement in rotor-side and grid-side converters of series-compensated DFIG-based wind farm," *IEEE Trans. Sustain. Energy*, vol. 6, no. 2, pp. 388–399, Apr. 2015.
- [18] P.-H. Huang, M. S. El Moursi, W. Xiao, and J. L. Kirtley, "Subsynchronous resonance mitigation for series-compensated DFIG-based wind farm by using two-degree-of-freedom control strategy," *IEEE Trans. Power Syst.*, vol. 30, no. 3, pp. 1442–1454, May 2015.
- [19] H. Liu, X. Xie, Y. Li, H. Liu, and Y. Hu, "Mitigation of SSR by embedding subsynchronous notch filters into DFIG converter controllers," *IET Gener., Transmiss. Distrib.*, vol. 11, no. 11, pp. 2888–2896, Mar. 2017.
- [20] F. Zhao, L. Wu, J. Zhang, X. Gao, H. Liu, H. Wang, and Y. Yang, "Suppression method of parallel-damping controller for DFIG," *J. Eng.*, vol. 2017, no. 13, pp. 880–884, 2017.
- [21] Y. Song and F. Blaabjerg, "Overview of DFIG-based wind power system resonances under weak networks," *IEEE Trans. Power Electron.*, vol. 32, no. 6, pp. 4370–4394, Jun. 2017.
- [22] J. Yao, X. Wang, J. Li, R. Liu, and H. Zhang, "Sub-synchronous resonance damping control for series-compensated DFIG-based wind farm with improved particle swarm optimization algorithm," *IEEE Trans. Energy Convers.*, vol. 34, no. 2, pp. 849–859, Jun. 2019. doi: 10.1109/TEC.2018.2872841.
- [23] M. A. Mahmud, H. R. Pota, M. Aldeen, and M. J. Hossain, "Partial feedback linearizing excitation controller for multimachine power systems to improve transient stability," *IEEE Trans. Power Syst.*, vol. 29, no. 2, pp. 561–571, Mar. 2014.
- [24] M. A. Chowdhury, M. A. Mahmud, W. Shen, and H. R. Pota, "Nonlinear controller design for series-compensated DFIG-based wind farms to mitigate subsynchronous control interaction," *IEEE Trans. Energy Convers.*, vol. 32, no. 2, pp. 707–719, Jun. 2017.
- [25] M. A. Chowdhury and G. M. Shafiullah, "SSR mitigation of series-compensated DFIG wind farms by a nonlinear damping controller using partial feedback linearization," *IEEE Trans. Power Syst.*, vol. 33, no. 3, pp. 2528–2538, May 2018.
- [26] J. Han, "From PID to active disturbance rejection control," *IEEE Trans. Ind. Electron.*, vol. 56, no. 3, pp. 900–906, Mar. 2009.
- [27] M. A. Chowdhury, A. H. M. Sayem, W. Shen, and K. S. Islam, "Robust active disturbance rejection controller design to improve low-voltage ride-through capability of doubly fed induction generator wind farms," *IET Renew. Power Gener.*, vol. 9, no. 8, pp. 961–969, Nov. 2015.



YANHUI XU was born in Heilongjiang, China, in 1978. He received the B.S. degree in thermal dynamic engineering, and the M.S. and Ph.D. degrees in electrical engineering from North China Electric Power University, in 2001, 2004, and 2010, respectively. His research interest includes power system stability and control and load modeling.



SHIMENG ZHAO was born in Liaoning, China, in 1994. She received the B.S. degree in electrical engineering and automation from North China Electric Power University, Beijing, in 2017, where she is currently pursuing the master's degree.

Her research field is about power system stability and sub-synchronous oscillations of the wind power.

...